Water dissociation on a defective MgO(100) surface: Role of divacancies

Benedicte Ealet,[1] Jacek Goniakowski,[1,2] and Fabio Finocchi[2]
[1]*Centre de la Recherche sur les Mécanismes de la Croissance Cristalline-CNRS Université de la Mediterranée, Campus de Luminy, 13288 Marseille, France*
[2]*Groupe de Physique des Solides, Universités Paris 6-7 and UMR CNRS 7588, 140, rue de Lourmel, 75015 Paris, France*
(Received 12 May 2003; revised manuscript received 5 March 2004; published 21 May 2004)

Surface divacancy at MgO(100) and its reactivity with water are studied by first-principles simulations. Among the most frequent point defects at MgO(100), the divacancy is estimated to be stable with respect to the formation of neutral oxygen and magnesium vacancies in moderate O environments. A single water molecule dissociates spontaneously at the divacancy. The final product of this exothermic reaction consists of a surface Mg vacancy with two adsorbed hydrogens—the (V_{Mg},2H) complex—which shows peculiar atomic and electronic structures. In particular, the stretching frequencies of the hydroxyl groups are downshifted noticeably, which can explain recent infrared data collected on wet MgO powders. The trend towards an aggregation of the brucite-like intrusions (V_{Mg},2H) is pointed out in relation with the complex behavior of the MgO(100) surface upon exposure to water.

DOI: 10.1103/PhysRevB.69.195413 PACS number(s): 73.20.Hb, 71.15.Pd, 82.65.+r, 82.30.Lp

I. INTRODUCTION

Most oxide surfaces react readily with water and become partially covered with water molecules or hydroxyl groups upon exposure to air under ambient conditions, with important consequences for surface processes such as catalysis and gas sensing. Whereas it is widely accepted that binding between molecular water and most oxide surfaces is dominated by electrostatic effects, namely the interaction of the H_2O electric dipole with the surface ions, a comprehensive understanding of the mechanisms by which dissociative adsorption occurs, the role of surface defects such as vacancies or steps, and the interaction between the adsorbed molecules is still lacking.[1]

As a model substrate, MgO has been one of most widely studied oxides. Although a considerable experimental and theoretical effort has gone into the study of H_2O adsorption on MgO(100), a clear picture has yet to emerge. The ambiguity regarding water dissociation, in particular, still constitutes a challenge.[1] Infrared spectra taken on MgO powders exposed to water[2] show the signatures of hydroxyl groups. Recently, a convincing experimental proof of water dissociation has been reported.[3] However, the preparation of the surface and the ambient water pressure and temperature plays a major role on surface hydroxylation. LEED and photoemission data showed two distinct behaviors on low defect density MgO(100) surfaces, which were interpreted as water being chemisorbed preferentially at defect sites, and then on terraces, for increasing coverage.[4] The defects were assumed to be mainly steps on cleaved surfaces, apart from the Ar^+-sputtered surfaces, which should contain point defects as well.[5] Nevertheless, terraces may mask the activity of a low concentration of point defects. Repeated water adsorption-desorption cycles on poly-crystalline samples of MgO showed a progressive inhibition towards water dissociation,[6] which was interpreted as due to the saturation of defects.

From the theoretical point of view, it is well established that the outcome of the water–surface interaction does depend on the orientation,[7–9] and that extended defects such as steps and kinks favor water dissociation.[10–12] Such a behavior can be linked to the more basic (acidic) character of under-coordinated O (Mg) atoms.[7,13] More generally, the interplay between the adsorption mode and energy, as well as the relation of the structural and vibrational properties of the adsorbed groups to the local environment of the adsorption sites, have been admitted. However, only recently it has become clear that an accurate modeling of the precise structural and electronic characteristics of the substrate, adequate boundary conditions, and a realistic treatment of the intermolecular interactions, are needed to account for the experiments with sufficient accuracy. For example, contrary to a common opinion gained from model calculations that perfect MgO(100) does not dissociate water, recent first-principles calculations[14–18] showed that a mixed molecular and dissociative water adsorption takes place at 1 ML coverage, as a result of interactions between the co-adsorbed molecules. *Ab initio* calculations of MgO clusters embedded in a dielectric continuum suggested that water dissociation at flat MgO(100) terraces may be stabilized at the MgO–water interface by the polarization of the surrounding molecules.[19]

Theoretical studies of the role of the precise surface morphology on the thermodynamics and kinetics of water dissociation, which are relevant for a better understanding of the experiments, focused more on the role of extended than point defects. A semi-empirical calculation of the energetics of adsorbed water and hydroxyl groups on mono-atomic steps, O (F_s) and Mg (V_{Mg_s}) surface vacancies, has recently appeared.[20] Very little is known on water dissociation at MgO divacancies, which may in principle exist in non-negligible concentrations at the (100) surface. In fact, unlike others defects, divacancies do not modify the surface stoichiometry and are not detected by many experimental techniques. Nevertheless, when an electron is trapped, for instance after the adsorption of a well chosen probe molecule,

 ©2004 The American Physical Society

such defects can be monitored by electron paramagnetic resonance spectroscopy.[21,22]

In line with our previous works on the interaction of water with MgO,[14,16,23] the aim of the present study is to provide a first-principles description of the local minima and transition states for the interaction of a H_2O molecule with a divacancy at the MgO(100) surface, in the limit of very low water coverage. The coherency of the computational approach makes possible a comparative analysis of the adsorption of water on the O vacancy and the MgO divacancy, the characterization of the dissociation products and the study of their properties with respect to those of analogous species adsorbed on the perfect surface.

The paper is organized as follows: first, we summarize the characteristics of an isolated divacancy on the MgO(100) surface. Then, we present the energetic and structural results obtained for the molecular and dissociative channels of water adsorption on the divacancy, which results in the formation of a (V_{Mg},2H) complex. We also describe the structural and vibrational characteristics of the surface hydroxyl groups, compare them to those calculated for OH^- groups in other surface environments, and discuss our results in the light of existing models for MgO surface sites able to dissociate water. Finally, the question of the interaction between the (V_{Mg},2H) complexes at higher coverage is briefly addressed.

II. COMPUTATIONAL SETTINGS

First-principles simulations are carried out within the density functional theory (DFT) in the generalized gradient approximation (GGA) for the exchange and correlation energy.[24,25] We use norm-conserving, separable pseudopotentials,[26,27] including the *s*, *p*, and *d* projectors for O and Mg, and *s* and *p* projectors for H. Plane waves of kinetic energy up to 25 Hartree are used for expanding the Kohn–Sham orbitals, ensuring a convergence of the total energy of the isolated water molecule and of the cohesive energy of bulk MgO to within 30 and 10 meV, respectively. The present approach has already proven its adequacy for an accurate treatment of defects on oxide surfaces,[28] of hydrogen bonds, and of water adsorption and dissociation.[14,16,23] We remind that for an isolated water molecule, the computed O–H bond length and the bond angle are equal to 0.976 Å and 103.5°. The calculated O–O distance in a water dimer is 2.89 Å (that estimated from microwave spectra is 2.98 Å[29]) and the dimer binding energy is (18 ± 1) kJ/mol (to be compared to the experimental estimates which range between 14 and 19 kJ/mol[30]). For the MgO(100) surface, we use the same slab approach as the one outlined in Refs. 28 and 23. The supercell consists of a four-layer-thick MgO(100) slab separated by an equivalent vacuum thickness. The $(2\sqrt{2}\times2\sqrt{2})$ surface unit cell is sampled with the $\overline{\Gamma}$ point. The surface defects and the adsorbed molecules are placed on one side of the slab only. In the geometry optimization procedure, all the atoms except those in the fourth MgO layer are mobile. Apart from the constrained optimization runs, the residual atomic forces in the final geometries do not exceed 10 meV/Å.

In the present study we consider a single surface divacancy and a single water molecule within the $(2\sqrt{2}\times2\sqrt{2})$ surface cell, which corresponds to a $\frac{1}{8}$ coverage of water molecules regularly arranged. The distance between their periodic images is of $\simeq$9 Å. We have performed additional calculations on the isolated divacancy using a (4×4) surface unit cell (corresponding to a 12.0 Å distance between the periodic images), in order to estimate the effect due to the surface unit cell size. We have found that the calculated formation energy of divacancy changes by less than 2% only. (It is partially due to a compensation between an increasing contribution due to a more extended relaxation: +10%, and to a decreasing contribution due to a weaker direct, attractive interaction: −8%, as deduced from ''rigid'' calculations.) We have also verified that the difference of Mg–O bond length modifications around the vacancy estimated with the two unit cells does not exceed 1.5%.

We have estimated the vibrational frequencies of O–H bond stretch from the Morse curve fitted to the computed total energy E versus the O–H bondlength d_{OH}. The latter one has been obtained by performing a full structural relaxation at constrained d_{OH}, thus taking into account the interaction of the hydroxyl group with the substrate and the defect. In all cases we have used seven values of d_{OH}, spaced uniformly by 0.02 Å. A comparison between the experimental and the calculated frequencies of free H_2O and OH^- molecules reveals a systematic underestimate of about 200 cm^{-1}. Tests carried out on these two molecules indicate that shifts as large as 100 cm^{-1} come from the use of soft pseudopotentials, which could be avoided if a smaller cutoff radius for O is chosen. However, this would imply a twice as big energy cutoff and thus a significant increase of the computational burden. The remaining discrepancy with the experimental values may be ascribed to the use of the GGA approximation, which is known to underestimate the OH stretching frequencies in brucite and portlandite.[31] Nevertheless, the pseudopotential-induced differences of the structural and energetic characteristics is of the order of 1%, and the stretching frequency shift among the frequencies computed with the softer and the harder pseudopotentials is constant within precision of our estimation. For the V_{Mg_s} complex, a weak coupling between the two hydroxyls can be shown by direct diagonalization of the dynamical matrix involving the OH groups, which yields a splitting as large as few tens cm^{-1}, depending on the actual configuration. Such a small effect is comparable to the variation of the anharmonic components when passing from one OH bonding configuration to another. Therefore, in the following, we adopt the softer O pseudopotential and discuss frequency shifts rather than absolute values.

III. THE ISOLATED SURFACE DIVACANCY

The formation of a surface divacancy, denoted hereafter by T_s (from ''tub'' [32]), corresponds to the extraction of two neighboring Mg and O atoms from the outermost surface plane. According to our calculations, the T_s formation energy (see Table I) is equal to 2.95 eV. Larger formation energies

TABLE I. Computed reaction enthalpy $\Delta H_r^{(0)}$ in eV, at zero temperature. Zero-point effects are not included. For the first reaction, the experimental value is −10.24 eV.[33]

	$\Delta H_r^{(0)}$ (eV)
$Mg_{(c)} + \frac{1}{2} O_{2(gas)} \rightarrow MgO_{(c)}$	−9.7
$MgO(100) \rightarrow MgO(100) + T_s + MgO_{(c)}$	2.95
$MgO(100) \rightarrow MgO(100) + F_s + \frac{1}{2} O_{2(gas)}$	5.53

obtained in embedded cluster calculations (4.03 eV by HF,[32] 3.92 eV by DFT-B3LYP[22,34]) may probably be due to the limited size of clusters and to constraints on atomic relaxations in this kind of calculations.[22] The isolated F_s plus V_{Mg_s} point defects are by far less stable than the T_s one. Indeed, the computed energy released in the reaction $F_s + V_{Mg_s} \rightarrow T_s$ at the MgO(100) surface is equal to 4.20 eV. As it has been suggested,[32,35] the recombination of these two surface defects is thus expected on thermodynamical basis. However, to our knowledge, a *direct* evaluation of the relative stability of those surface point defects had not been performed so far. Since the $MgO(100) + T_s$ system is stoichiometric, while $MgO(100) + F_s$ and $MgO(100) + V_{Mg_s}$ are not, a meaningful comparison can only be done as a function of the excess oxygen chemical potential (i.e., with respect to a reservoir of gaseous O_2). The reader is referred to the literature[36,37] for a discussion of the formation energy of surface defects as a function of the actual stoichiometry. Our results for the formation energies of T_s and F_s at MgO(100) are summarized in Fig. 1. We see that, while in O-poor conditions (UHV conditions) the F_s center is favored, T_s is thermodynamically more stable for moderately rich O environments. Since it is always less stable than the perfect MgO(100) surface, the occurrence of the T_s defect should thus be linked to kinetic effects upon growth or surface–particle interaction, such as ion bombardment. This is consistent with recent first-principle calculations, which indicate that the MgO ad-molecule should hardly diffuse at room temperatures,[38] making the recombination reaction $MgO(100) + T_s + MgO_{(ad)} \rightarrow MgO(100)$ rather unlikely.

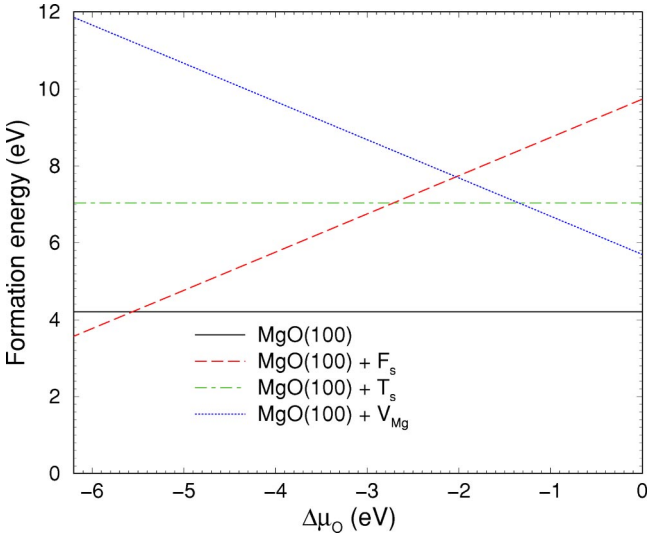

FIG. 1. (Color online) The computed free energies of formation of the T_s, F_s and V_{Mg_s} point defects are compared to the perfect MgO(100) surface as a function of the O excess chemical potential $\Delta\mu_O$—defined as μ_O—$1/2\mu_{O_{2(gas)}}$. $\Delta\mu_O$ is bounded from below by the formation energy of the MgO crystal with respect to the stable elemental phases (i.e., gaseous O_2 and crystalline Mg).

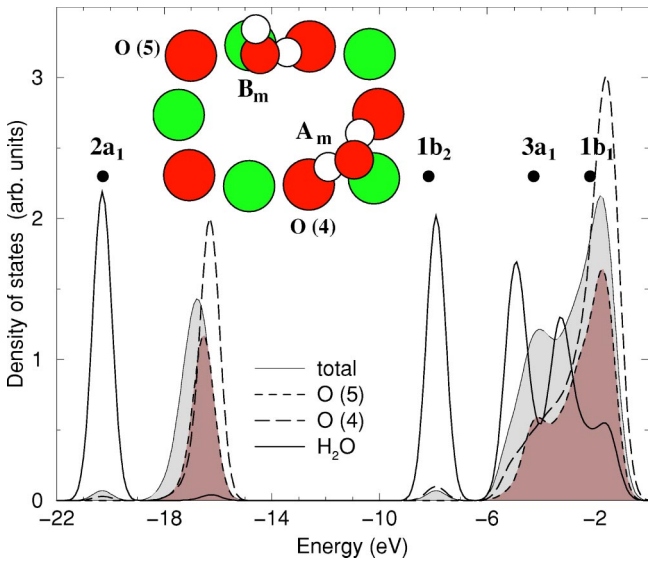

FIG. 2. (Color online) Densities of states (DOS) and top view of the atomic structure (inset) of an isolated water molecule physisorbed at a divacancy. The two different adsorption configurations, labeled A_m and B_m, give rise to almost superposable DOS. The surface magnesium and oxygen atoms are represented by large green and red circles respectively, whereas small white circles represent hydrogen atoms. As a reference, we present the energies of molecular orbitals of a free water molecule (dots) and DOS projected on two low-coordinated oxygen ions O(4) and O(5), as calculated without adsorbed water molecule.

The stoichiometry is the main distinction between the T_s and the F_s defects, and it is responsible for their qualitatively different electronic and structural properties, as well as their specific reactivity. Structural relaxation around a divacancy is non-negligible: the relaxation energy amounts to ≃3 eV (to be compared to 0.2 eV in the case of the F_s center), and the atomic in-plane displacements from their bulk-like equilibrium positions are of the order of 7% (to be compared to 1% on the clean surface and 3% around the F_s defect[28]), approaching what has been found on stepped MgO(100) surfaces.[39] The overall shape of the relaxed defect is clearly rounded and corresponds to a bond shortening for atoms at the divacancy edges, accompanied by a bond dilation for atoms in the corners (see Fig. 2). Among the former ones, the strongest effect is seen on the under-coordinated Mg ions, which experience 7% and 2% contractions of the bonds to their O neighbors in the surface plane and below, respectively. The relaxation of the under-coordinated anions is a little weaker, and the contraction amounts to 6% and 1%, for the in-plane and inter-plane Mg-O bonds, respectively. At

TABLE II. Adsorption energy and structural characteristics of an isolated water molecule physisorbed at the T_s center and on the perfect MgO(100) surface.

	A_m	B_m	Perfect surface
E_{ads} (eV)	0.67	0.45	0.42
$d_{\text{O-Mg}}$ (Å)	2.17	2.16	2.23
$d_{\text{O-H}}$ (Å)	0.99, 0.99	0.96, 0.96	0.96, 1.00
z_{O} (Å)	2.09	2.13	2.19
$d_{\text{H-O}_s}$ (Å)	1.86, 1.79	1.76	1.78

variance, the fivefold coordinated ions at the vacancy corners exhibit an elongation of the Mg–O distances (of about 11% and 4% for Mg and O ions, respectively) with their neighbors, which are fivefold coordinated, too. Nevertheless, we stress that the latter values are likely the most biased by the size of the surface unit cell.

Oxygen sites at the T_s corners [O(5)] have a full surface first coordination shell, while the edge sites [O(4)] are only fourfold coordinated. As a consequence, the nonbonding states of the O(4) atoms are up-shifted with respect to the clean surface valence band maximum by 0.3 eV. This can be attributed to a weakening of the Madelung field, which is only partially compensated by the contraction of the remaining O–Mg bonds.[39] The modifications of the DOS remain thus relatively small, and contrarily to the case of the neutral F_s center, no gap states are present and no electron delocalization in space regions off the atomic sites takes place.

Although the structural and electronic characteristics of the T_s defects may be thought as analogous to those of mono-atomic steps on MgO(100), it has been stressed in Ref. 32 that the electrostatic field at T_s displays a strong dissymmetry, being positive (negative) close to the missing Mg (O). This, and the spatial disposition of low-coordinated ions, point out the fourfold coordinated ions at T_s edges as the most promising for surface reactions.

IV. WATER ADSORPTION

Interaction of an isolated water molecule with the surface divacancy ($MgO(100)+T_s+H_2O_{(gas)}$) gives rise to stable atomic configurations in both molecular and dissociative adsorption modes. In the following, we discuss the corresponding structural and energetic characteristics, and estimate the energy barriers separating the different configurations.

A. Molecular adsorption

Table II and Figure 2 summarize the structural and electronic properties of an isolated water molecule physisorbed at a T_s center. For comparison, the corresponding results for water adsorption on the perfect MgO(100) surface are given in Table II.

The two alternative configurations of molecularly adsorbed water are significantly different. Although the configuration B_m happens to be quite similar to that of an isolated water molecule at the perfect MgO(100) surface, it corresponds to a plateau of the potential energy surface rather than to a minimum. The adsorbed molecule experiences very tiny forces (less then 50 meV/Å), which can be affected by the actual choice of the exchange and correlation energy. The adsorption is reinforced, regarding the hydrogen bonds (see $d_{\text{H-O}_s}$) as well as the interaction of the molecule dipole moment with the surface (see $d_{\text{O-Mg}}$). Both effects can be associated to the lower, fourfold coordination of the ions at the divacancy edge, as compared to the fivefold coordinated sites at the perfect surface. However, the overall increase of the adsorption energy remains relatively modest.

The configuration A_m is much more unusual. We notice the formation of two quasi-symmetric hydrogen bonds between the molecule and the surface anions and the resulting considerable increase of adsorption energy. The weakening and change of symmetry of the surface electrostatic field at the divacancy gives the adsorbed molecule more freedom and enables the creation of two hydrogen bonds, at variance with the perfect MgO(100) surface and with the configuration B_m, where only one hydrogen bond between the admolecule and the surface is formed.

However, differences between the two adsorbed configurations affect little their respective DOS. This is why in Fig. 2 we present the DOS corresponding to the A_m configuration only. With respect to the free water molecule, the main modification consists of a downshift of the $3a_1$ and $1b_1$ orbitals. The latter being much stronger as compared to molecular water adsorption on the perfect MgO(100) surface and on the F_s center,[23] they can be directly related to the increase of the surface-molecule interaction (see $d_{\text{O-Mg}}$). We also notice that the levels of fourfold coordinated O atom (up-shifted by 0.3 eV with respect to the perfect surface valence band), lower by 0.1 eV after water adsorption.

B. Dissociative adsorption

The two physisorbed configurations presented in the previous section exhibit a significantly different stability towards dissociation. The molecule in the B_m configuration dissociates spontaneously towards the surface complex denoted B_d in Fig. 3 and Table III. However, the actual value of the barrier, if there is any, might be very sensitive to different treatments of the exchange-correlation energy. The alternative dissociated configuration, denoted as A_d, can be reached from the molecular configuration A_m (the corresponding barrier is equal to $\simeq$1.6 eV) or from B_d, through an energy barrier of about 0.7 eV. As a reference, in Table III we present also the results obtained for the configuration in which one of the two H is bound to a fivefold coordinated oxygen site at the MgO(100) terrace. In this configuration, denoted hereafter as C_d, a single OH group remains at the vacancy.

Water dissociation at T_s is strongly exothermic–the largest calculated energy gain amounts to 2.96 eV. We notice that the energy gained in dissociating the water molecule compensates the formation energy of the T_s defect on the clean surface (2.95 eV). This is due to the conjunction of two factors: on one hand, for all three configurations, the oxygen, initially in the water molecule, replaces the missing O atom

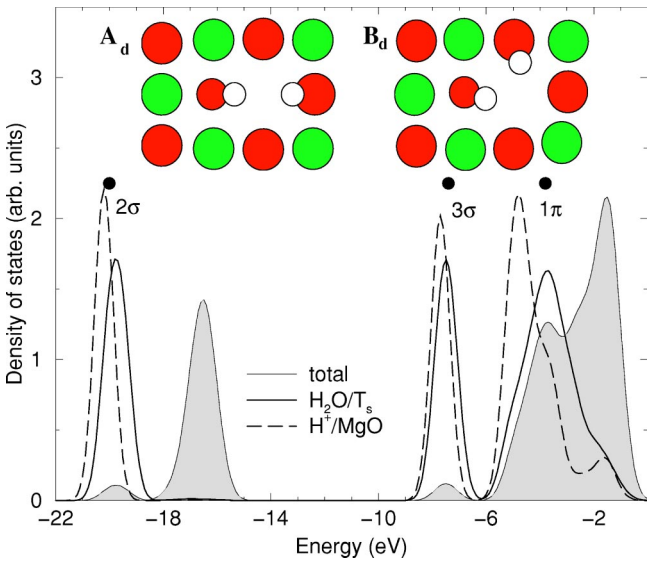

FIG. 3. (Color online) DOS and atomic structures (insets) of a water molecule dissociated at the divacancy. The two distinct configurations are labeled A_d and B_d. They give rise to similar DOS. As a reference we give the molecular levels of a free OH^- molecule (dots) and the DOS of H^+ adsorbed on a perfect MgO surface.

in the divacancy. On the other hand, the bonds formed between the hydrogen and the oxygen atoms at the vacancy edge are almost parallel to the surface plane (see z_H in Table III), so that the protons lie in the electrostatic trap left by the missing Mg cation. The electrostatic gain is thus an important contribution to the energy released in the divacancy hydroxylation. The dilated O–H bond (as compared to 0.963 Å in the calculated free OH^- molecule) reflects the competition between the covalent character of the OH bond and the effect of proton trapping by the electrostatic field of the V_{Mg} center. The slightly larger E_{ads} in the A_d configuration can be explained by the smaller repulsion between the H^+ in the vacancy, as revealed by the comparison of $d_{H\text{-}H}$ between A_d and B_d in Table III. These results are in line with a previous analysis of the electrostatic potential and its gradient close to the bare V_{Mg} defect at MgO(001).[40]

We notice, however, that the above effects influence only little the electronic structure and that both A_d and B_d configurations give rise to an equivalent DOS (Fig. 3), which resembles closely that of a free OH^- molecule. The differences between the DOS of OH groups issued from water dissociation at the divacancy and of a H^+ adsorbed on perfect MgO(100) concern mainly the 1π orbital and are due to a different hybridization of the $2p$ orbitals of the surface oxygen ion. We also notice a small overall shift due to a slightly weakening of the electrostatic potential at the oxygen ions in the case of OH groups at the vacancy edge.

TABLE III. Adsorption energy and structural parameters of the three configurations of water molecule dissociated at an isolated surface divacancy.

	A_d	B_d	C_d
E_{ads} (eV)	2.96	2.83	2.55
$d_{O\text{-}Mg}$ (Å)	2*2.21, 2.10, 2.24	2*2.14, 2.26, 2.32	2*2.19, 2.14, 2.23
$d_{O\text{-}H}$ (Å)	0.97	0.97	-
z_H (Å)	0.35, 0.35	0.35, 0.35	0.29
$d_{H\text{-}O_s}$ (Å)	0.967	0.969	0.970
$d_{H\text{-}H}$ (Å)	2.44	2.07	-

The A_d and B_d configurations issued from the water dissociation at the surface divacancy can be seen as two distinct realization of the (V_{Mg},2H) complex, according to the reaction: $MgO(100)+T_s+H_2O_{(gas)} \rightarrow MgO(100)+(V_{Mg},2H)$. In principle, such a complex can alternatively be obtained by a homolytic dissociation of a molecular hydrogen at the surface Mg vacancy: $MgO(100)+V_{Mg}+H_{2(gas)} \rightarrow MgO(100)+(V_{Mg},2H)$. Similarly to these reactions, the replacement of the calcium ions by two protons each has been recently investigated theoretically on the CaO(100) surfaces.[41]

In spite of the relevance of H_2 dissociation for catalysis, little is known on the role of V_{Mg} centers. The barrier for dissociation calculated by *ab initio* quantum chemical method has been estimated to 1.7 eV, leading to the formation of two OH bonds almost parallel to the surface plane, and with lengths of 1.0 Å.[42] Such a configuration is clearly similar to our (V_{Mg},2H) complex. However, since Mg vacancies should seldom appear on the clean MgO(100) surface at thermodynamic equilibrium (see Fig. 1), we think that the hydroxylation of divacancies is actually the main process able to produce (V_{Mg},2H) complexes.

In order to better understand the properties of such a surface complex, we remind that a neutral V_{Mg} center is characterized by two holes distributed over the neighboring oxygen ions, which results in a lower electronic occupation of anions.[43] As a consequence, this surface defect acts as a strong electron acceptor. This, together with the argument based on surface electrostatics (restitution of the positive charge in place of the missing cation), results in a strong preference for a homolytic dissociation of H_2. The corresponding dissociation energy $[E(V_{Mg},2H)-E(V_{Mg})-E(H_2)]$ is equal to 5.28 eV/hydrogen molecule, in good agreement with the value of 5.4 eV reported in Ref. 42. It confirms the stability of the (V_{Mg},2H) complex, for which we thus do not expect a desorption of molecular hydrogen, as it was shown to be the case for water recombination with an oxygen vacancy:[23] $MgO(100)+F_s+H_2O \rightarrow MgO(100)+H_{2(gas)}$.

V. THE (V_{Mg},2H) COMPLEX

In this section, we focus on the (V_{Mg},2H) complexes issued from the interaction of water molecules with the surface T_s centers. In particular, we discuss their diffusion at the surface, and show that there is an attractive interaction between them. We also study the high-frequency part of the vibrational spectrum, in order to provide an easily recognizable fingerprint for the occurrence of (V_{Mg},2H) on real wet MgO(100) samples.

A. Diffusion

In the previous section, we characterized the structural properties of the (V_{Mg},2H) complex, yet one may wonder

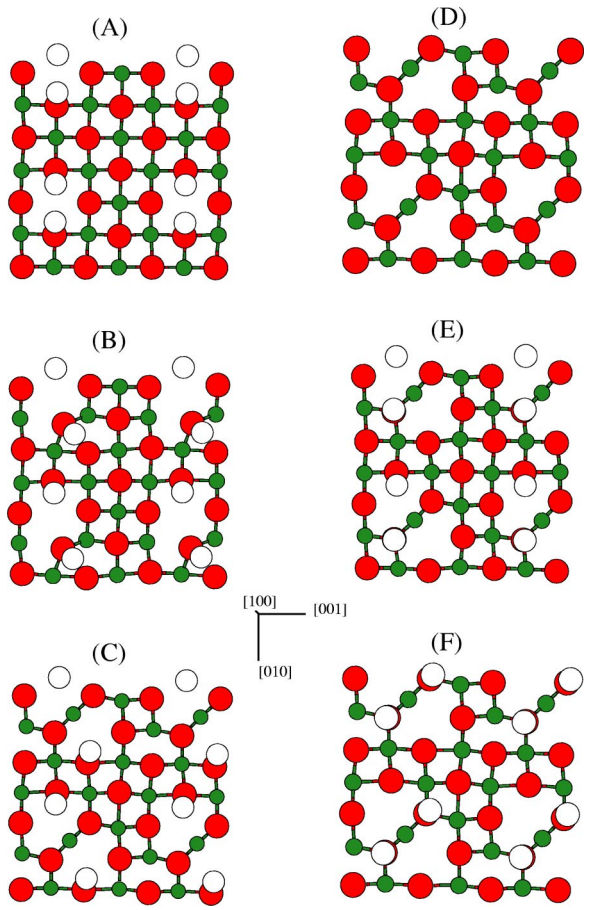

FIG. 4. (Color online) Top view of selected configurations along the computed diffusion path of the (V_{Mg},2H) complex. (a) A_d initial configuration, point group C_{2v}. (b) Proton diffusion, accompanied by the motion of the Mg atom. (c) saddle-point configuration, point group C_2. (d) saddle-point configuration for the V_{Mg_s} diffusion at the dry MgO(100) surface. The (e) and (f) configurations represent additional saddle points, as discussed in the text. The effect of the periodic boundary conditions has been pointed out by drawing some of the periodic images outside the two-dimensional unit cell.

whether it can propagate on the surface. Although its diffusion should likely depend on the surface stoichiometry, the presence of another point or extended defects and, more importantly, on the actual water coverage, a first answer to the question can be given by looking at the energy barrier for the isolated (V_{Mg},2H) complex to diffuse at the flat MgO(100) surface.

Even for such a model system, the diffusion is not a simple process, but rather involves multiple barriers that correspond to distinct physical events. The first half of the path with the smallest barrier that we find through constrained molecular dynamics runs[44] is sketched in Figs. 4(a)–4(c). The second half is symmetric and has not been drawn. It can be described as follows: Starting from configuration A_d [Fig. 4(a)], one of the protons raises upon the surface plane and binds to a neighboring oxygen [Fig. 4(b)]. The corresponding energy barrier is estimated to $\simeq$1.1 eV. At the same time, the Mg atom moves toward the V_{Mg_s} site, *below* the surface plane. The saddle point configuration [Fig. 4(c), $\simeq$1.3 eV above the energy of the most stable A_d configuration] is remarkably symmetric: the magnesium is exactly midway between two V_{Mg_s} sites, each close to a hydroxyl group. The magnesium is about 0.07 Å under the average position of the surface layer, while the two oxygen neighbors are pushed up by 0.30 Å, with Mg–O bond lengths equal to 1.83 Å. Such a rather short Mg–O bond (to be compared to 2.14 Å, as computed in bulk MgO) correlates with the reduced Mg and O coordination numbers (2 and 4, respectively). Accordingly, the diffusing Mg can form rather short bonds, without being forced to move below the surface plane considerably, so to limit the elastic stress accompanying its diffusion. For the sake of comparison, this energy barrier is close to that computed for the diffusion of V_{Mg_s} at the clean MgO(100) surface [see Fig. 4(d)], which amounts to about 1.1 eV.

In this respect, it has to be pointed out the indirect, but important, role played by the OH groups. Indeed, if the diffusing Mg passes one or two surface hydroxyl groups, the corresponding Mg–O equilibrium bond length would tend to increase considerably but steric effects prevent it from doing that, thus provoking a rather big and long-range elastic stress. For instance, starting from the A_d configuration [Fig. 4(a)], but constraining the Mg midway between an oxygen atom and a OH group (still letting its vertical position free) and optimizing all remaining atomic coordinates, we obtain the (e) configuration in Fig. 4. Its energy is $\simeq$1.9 eV higher than (a) and $\simeq$0.6 eV higher than the saddle point (c). When the Mg is put midway between two OH groups [Fig. 4(f)], which can be obtained starting from the B_d metastable configuration in Fig. 3, the energy raises more than 3 eV, much higher than our computed saddle point energy. Once the saddle point represented in Fig. 4(c) is attained, the next step for a complete migration of the (V_{Mg},2H) complex towards a new equilibrium configuration (C_d first, then A_d or B_d as in Fig. 3, after the proton diffusion) is the concerted diffusion of the adsorbed proton and the magnesium atom, along a sequence that is symmetric with respect to the (a) to (c) path.

Quantum effects on the proton motion, which were not taken into account in our simulations, should modify such a path considerably and decrease the energy barriers along it. Furthermore, the consideration of larger unit cells would relax some of the mechanical stress accompanying the (V_{Mg},2H) diffusion. For all these reasons, the values provided here, and in particular the lowest diffusion barrier of 1.3 eV, can be considered as an upper estimate on the energy barriers along the diffusion of the (V_{Mg},2H) complex.

B. Mutual interaction

In this section, we focus on the mutual interaction between the (V_{Mg},2H) complexes issued from the interaction of a water molecule with a T_s center. It is worth stressing that their composition is equivalent to that of a brucite ($Mg(OH)_2$) unit embedded in the surface layer of MgO(100). For an arbitrary concentration, this equivalence can be summarized as follows:

$$l\mathrm{MgO}+m(V_{\mathrm{Mg}},2\mathrm{H})\leftrightarrow(l-2m)\mathrm{MgO}+m\mathrm{Mg(OH)}_2.$$

It is clear that the largest surface concentration $n_s = m/l$ of the (V_{Mg},2H) complexes is equal to one-half ($l-2m=0$), and corresponds to the formation of a layer of $Mg(OH)_2$ stoichiometry on top of a stoichiometric MgO(100) surface. If considered as point defects, the concentration-dependent formation energy $E_f(n_s)$ of (V_{Mg},2H) can be deduced from the following reactions:

$$\mathrm{MgO}(100) + n_s \mathrm{H_2O_{(gas)}} \rightarrow \tag{1}$$

$$\mathrm{MgO}(100) + n_s[\mathrm{T}_s + \mathrm{MgO_{(c)}} + \mathrm{H_2O_{(gas)}}] \rightarrow \tag{2}$$

$$\mathrm{MgO}(100) + n_s(\mathrm{V_{Mg}},2\mathrm{H}) + n_s \mathrm{MgO_{(c)}}. \tag{3}$$

Comparing the total energies of the final and initial states we obtain

$$n_s E_f(n_s) = E[\mathrm{MgO}(100) + n_s(\mathrm{V_{Mg}},2\mathrm{H})] + n_s E[\mathrm{MgO_{(c)}}] - E[\mathrm{MgO}(100)] - n_s E[\mathrm{H_2O_{(gas)}}]. \tag{4}$$

Reaction (1) corresponds to the formation of n_s T_s centers on the MgO(100) surface (for $n_s = 1/8$ it amounts to 2.95 eV). Reaction (2) represents the dissociative adsorption of water on each of them (for $n_s = 1/8$ it amounts to -2.96 eV). Therefore, according to Eq. (4), the formation energy $E_f(n_s)$ of the brucite-like intrusions can also be obtained as a difference between the dissociation energy of water on the T_s center, diminished by the formation energy of the latter one. For the lowest surface concentration that we consider ($n_s = 1/8$), which approaches the situation of an isolated brucite intrusion (see Fig. 3), the calculated formation energy is almost null [$E_f(1/8) = -0.01$ eV], within our numerical accuracy. This result can be compared to the replacement energy of a CaO unit by a water molecule, which amounts to -0.44 eV on the CaO(100) surface.[41]

In order to estimate the character of the interaction between the brucite-like intrusions we performed calculations corresponding to $n_s = 1/2$, in the same two-dimensional unit cell. The computed atomic structure of this configuration [due to its resemblance to a distorted $(11\bar{2}0)$ brucite layer, hereafter we refer to it as 1ML $Mg(OH)_2$] is represented in Fig. 5. The formation energy $E_f(1/2)$ calculated for this structure amounts to -0.68 eV, which corresponds to an endothermic reaction. The difference $E_f(1/8) - E_f(1/2) \simeq 0.7$ eV can be thus considered as a measure of a strongly attractive character of the interaction between the (V_{Mg},2H) complexes.

C. Vibrational characteristics

In order to get an insight on the spectroscopic signature of the (V_{Mg},2H) complex, we have estimated the vibrational frequency of the stretching mode of the OH bonds in the A_d, B_d, and C_d configurations. The harmonic frequencies ω were obtained from the fit of a Morse curve to the calculated total energy as a function of oxygen–proton bondlength $d_{O\text{-}H}$. In

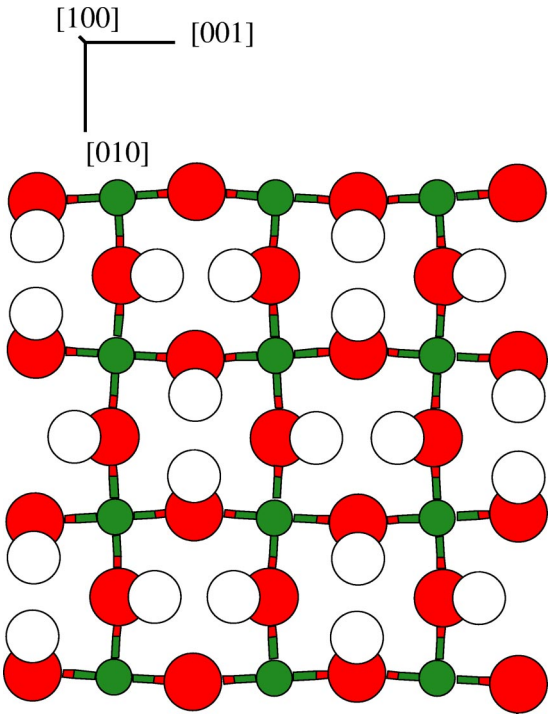

FIG. 5. (Color online) Top view of the outermost layer of $n_s = 1/2$ (V_{Mg},2H) complexes on the MgO(100) surface (''distorted brucite $(11\bar{2}0)$ layer'').

Fig. 6 we present the dependence of the calculated frequency shift $\Delta\omega$ on the modification of the equilibrium bond length of the corresponding hydroxyl group, $\Delta d_{O\text{-}H}$. We use the data obtained for a free OH^- molecule as a reference: $\Delta\omega = 0$ and $\Delta d_{O\text{-}H} = 0$. For the sake of comparison we add the results obtained for an isolated H^+ at the oxygen site of the perfect MgO(100) surface and for an isolated OH^- group bridging two magnesium sites of the same surface. As already pointed out,[45] there is a relatively small frequency shift

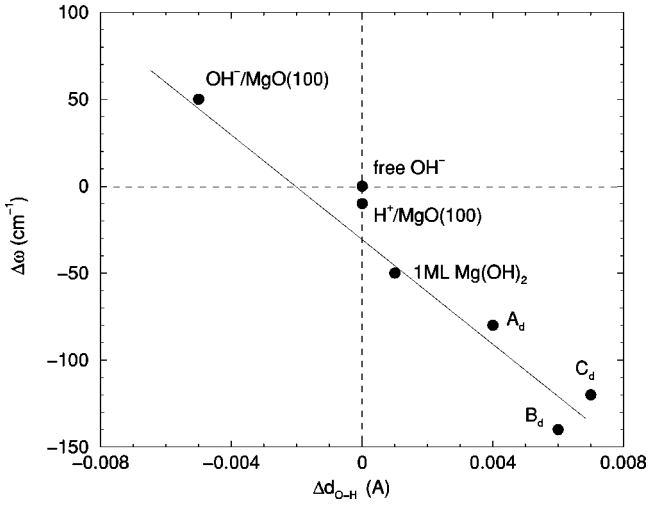

FIG. 6. (Color online) Frequency shifts $\Delta\omega$ as a function of modification of the equilibrium bond length of the corresponding hydroxyl group, $\Delta d_{O\text{-}H}$, plotted with respect to the free OH molecule.

between the free OH^- molecule and isolated protons or OH groups adsorbed on the perfect MgO(100) surface. Conversely, the stretching frequencies of the OH groups in an isolated (V_{Mg},2H) complex are systematically downshifted. According to our calculations, this shift can amount to as much as 150 cm^{-1} (conf. B_d).

It is clear from Fig. 6 that the principal reason for this frequency modification is to be traced back to the dilation of the corresponding OH bond length. In fact, our results reveal a proportionality between these two quantities that is valid in a relatively large range of $\Delta d_{O\text{-}H}$. Such a relation has already been suggested on a basis of analytical models and calculations, either semi-empirical or based on various first-principles hamiltonians, for differently coordinated surface OH groups.[7,46] In the present case, however, the strong dilation of OH bondlength (for the most shifted, B_d and C_d configurations, the calculated $\Delta d_{O\text{-}H}$ is of the order of -1%) is to be related to the interaction with the electrostatic environment of the Mg vacancy, rather than to a lower coordination of the vacancy-edge site (which in fact would produce a shortening of OH distance), whereas, it results from the combination of two electrostatic effects: proton trapping by the magnesium vacancy and repulsion between the two protons (compare the corresponding $d_{H\text{-}H}$ in Table III). The latter can be held responsible for the considerably different $\Delta d_{O\text{-}H}$ (and thus $\Delta\omega$) found for A_d and C_d configurations. The finer modifications of the calculated frequency shift (B_d versus C_d configurations) are due also to a different coupling between the vibration modes of the two hydroxyl groups.

These results clearly show that the distinctive features of the electrostatic field around point defects at the MgO surface can be relevant enough to dominate the characteristics of surface OH radicals and question the general validity of simple models relating $\Delta\omega$ merely to the coordination number of the OH radicals. Moreover, the relatively low vibration frequencies that are associated with the (V_{Mg},2H) complex should be detectable experimentally well out of the usual structures located around and above 3500 cm^{-1}. In fact, recent results of hydride oxidation of MgO by O_2 or H_2O show a distinctive feature at 3294 cm^{-1}, which the authors associate with a very strong—so far unknown—proton acceptor.[47] The same feature is observed at MgO powders exposed simultaneously to H_2 and O_2.[48] The present results suggest that (V_{Mg},2H) complexes could constitute a model of the site responsible for such low frequencies.

VI. SUMMARY AND CONCLUSIONS

The main results of our study on interaction of an isolated water molecule with a divacancy on the (100) surface of MgO by first-principles methods can be summarized as follows:

Water dissociates spontaneously on T_s. The final state, in which the oxygen ion of the water molecule recombines with the divacancy, is equivalent to a H_2 molecule dissociated at a surface magnesium vacancy, and involves two symmetric surface OH groups. Such a (V_{Mg},2H) complex is characterized by a peculiar electrostatic field and is much more stable against hydrogen desorption than H adsorbed on perfect MgO(100) terraces.

The (V_{Mg},2H) *complex on the MgO(100) surface shows noticeable and easily identifiable vibration modes for the OH groups*. Conversely to the usual arguments that predict a systematic reinforcing of the OH bond and a frequency upshift as the coordination decreases,[2] we have shown that, despite the reduced O coordination, in the (V_{Mg},2H) complex the electrostatic effects dominate, resulting in a well pronounced decrease of the OH stretching frequency with respect to the perfect surface. This effect could explain the origin of the unusual infrared signatures obtained recently on MgO powders exposed to oxygen and hydrogen.[48]

Although the occurrence of T_s *point defects is not favorable on clean MgO(100) terraces in thermodynamic equilibrium, it can become competitive upon hydroxylation*. Indeed, the energetic cost of creating a divacancy is almost completely compensated by the energy released in the dissociation of a water molecule. Since the (V_{Mg},2H) complexes show an attractive interaction, that can make them even more competitive at high concentrations. This fact stresses the importance of accounting for the surface–adsorbate and the adsorbate–adsorbate interaction on the same level, as the thermodynamic and kinetic properties of the resulting surface configurations can be largely affected.

As far as the stoichiometry is concerned, *the* (V_{Mg},2H) *complex corresponds to a local brucite-like intrusion on the MgO(100) surface*. Our simulations suggest the possibility for such intrusions to form brucite-like clusters that may have a precursor role in the surface transformation upon repeated exposure to water.[49]

The formation of the (V_{Mg},2H) complex is therefore relevant in two respects: First, the Mg vacancy can play a fundamental role since, being a very strong proton acceptor, it opens the way to the hydroxylation of the MgO(100) surface. Its stability must also be reconsidered in humid environments. Second, the complex could act as a precursor to the dissociation and dissolution of MgO through the formation of brucite-like intrusions. The differences in bond lengths and coordination numbers for the O atom in such OH groups can be detected experimentally, and we point out that simple molecules, such as H_2O, can constitute effective probes for point defects on magnesium oxide surfaces.

ACKNOWLEDGMENTS

We are grateful to François Bottin and Dominique Costa for fruitful discussions. Most calculations were carried out on the NEC-SX5 and on the IBM-SP4 at the CNRS-IDRIS computational center, under project Nos. 020732 and 024089. A part of this study was supported by the COST D19 action and GDR DFT.

[1] M. A. Henderson, Surf. Sci. Rep. **46**, 1 (2002).
[2] E. Knozinger, K. H. Jacob, S. Singh, and P. Hoffmann, Surf. Sci. **290**, 388 (1993).
[3] Y. D. Kim, R. M. Lynden-Bell, A. Alavi, J. Stulz, and D. W. Goodman, Chem. Phys. Lett. **352**, 318 (2002).
[4] P. Liu, T. Kendelewicz, G. E. Brown, and G. A. Parks, Surf. Sci. **412/413**, 287 (1998).
[5] P. Liu, T. Kendelewicz, G. E. Brown, and G. A. Parks, Surf. Sci. **412/413**, 315 (1998).
[6] D. Abriou and J. Jupille, Surf. Sci. **430**, L527 (1999).
[7] J. Goniakowski and C. Noguera, Surf. Sci. **330**, 337 (1995).
[8] N. H. de Leeuw and S. C. Parker, Phys. Rev. B **58**, 13901 (1998).
[9] K. Refson, R. A. Wogelius, and D. G. Fraser, Phys. Rev. B **52**, 10823 (1995).
[10] C. A. Scamehorn, N. M. Harrison, and M. I. McCarty, J. Chem. Phys. **101**, 1547 (1994).
[11] W. Langel and M. Parrinello, J. Chem. Phys. **103**, 3240 (1995).
[12] J. A. Mejias, A. J. Berry, K. Refson, and D. G. Fraser, Chem. Phys. Lett. **314**, 558 (1999).
[13] F. Finocchi and C. Noguera, in *Acid-Base Interactions*, edited by K.L. Mittal (VSP, Utrecht, 2000), Vol. II.
[14] L. Giordano, J. Goniakowski, and J. Suzanne, Phys. Rev. Lett. **81**, 1271 (1998).
[15] M. Odelius, Phys. Rev. Lett. **82**, 3919 (1999).
[16] L. Giordano, J. Goniakowski, and J. Suzanne, Phys. Rev. B **62**, 15406 (2000).
[17] L. Delle Site, A. Alavi, and R. M. Lynden-Bell, J. Chem. Phys. **113**, 3344 (2000).
[18] J. H. Cho, J. M. Park, and K. S. Kim, Phys. Rev. B **62**, 9981 (2000).
[19] M. A. Johnson, E. V. Stefanovich, T. N. Truong, J. Gunster, and D. W. Goodman, J. Phys. Chem. B **103**, 3391 (1999).
[20] B. Ahlswede, T. Homann, and K. Jug, Surf. Sci. **445**, 49 (2000).
[21] G. Piranello, C. Pisani, A. D'Ercole, M. Chiesa, M. C. Paganini, E. Giamello, and O. Diwald, Surf. Sci. **494**, 95 (2001).
[22] D. Ricci, G. Pacchioni, P. V. Sushko, and A. L. Shluger, J. Chem. Phys. **117**, 2844 (2002).
[23] F. Finocchi and J. Goniakowski, Phys. Rev. B **64**, 125426 (2001).
[24] A. D. Becke, Phys. Rev. A **38**, 3098 (1988).
[25] J. P. Perdew and Y. Wang, Phys. Rev. B **33**, 8800 (1986).
[26] N. Troullier and J. L. Martins, Phys. Rev. B **43**, 1993 (1991).
[27] L. Kleinman and D. M. Bylander, Phys. Rev. Lett. **48**, 1425 (1982).
[28] F. Finocchi, J. Goniakowski, and C. Noguera, Phys. Rev. B **59**, 5178 (1999).
[29] T. R. Dyke and J. S. Muenter, J. Phys. Chem. **60**, 2929 (1973).
[30] L. A. Curtiss, D. J. Frurip, and M. Blander, J. Chem. Phys. **71**, 2703 (1979).
[31] P. Baranek, A. Lichanot, R. Orlando, and R. Dovesi, Chem. Phys. Lett. **340**, 362 (2001).
[32] L. Ojamäe and C. Pisani, J. Chem. Phys. **109**, 10984 (1998).
[33] *CRC Handbook of Chemistry and Physics*, edited by D.R. Lide (CRC, Boston, 1999).
[34] P. V. Sushko, A. L. Shluger, and C. R. A. Catlow, Surf. Sci. **450**, 153 (2000).
[35] A. Bogicevic and D. R. Jennison, Surf. Sci. **437**, L741 (1999).
[36] G.-X. Qian, R. M. Martin, and D. J. Chadi, Phys. Rev. B **38**, 7649 (2003).
[37] C. H. Park and D. J. Chadi, Phys. Rev. B **49**, 16467 (1994).
[38] G. Geneste, J. Morillo, and F. Finocchi, Appl. Surf. Sci. **188**, 122 (2002).
[39] J. Goniakowski and C. Noguera, Surf. Sci. **340**, 191 (1995).
[40] A. D'Ercole, A. M. Ferrari, and C. Pisani, J. Chem. Phys. **115**, 509 (2001).
[41] N. H. de Leeuw and J. A. Purton, Phys. Rev. B **63**, 195417 (2001).
[42] S. A. Pope, M. F. Guest, I. H. Hillier, E. A. Colbourn, W. C. Mackrodt, and J. Kendrick, Phys. Rev. B **28**, 2191 (1983).
[43] A. M. Ferrari and G. Pacchioni, J. Phys. Chem. **99**, 17010 (1995).
[44] In MD runs, the atoms are treated as classical particles. Quantum effects on the motion of protons, which should decrease the energy barriers and may modify the lowest-energy path, are thus neglected. However, the computational burden of first-principles calculations within a path-integral formulation, see e.g., D. Marx and M. Parrinello, J. Chem. Phys. **104**, 4077 (1996), is too big.
[45] M. Alfredsson and K. Hermansson, Mol. Simul. **28**, 663 (2002), and references therein.
[46] M. Merawa, B. Civalleri, P. Ugliengo, Y. Noel, and A. Lichanot, J. Chem. Phys. **119**, 1045 (2003).
[47] O. Diwald, M. Sterrer, and E. Knözinger, Phys. Chem. Chem. Phys. **4**, 2811 (2002).
[48] O. Diwald and E. Knözinger, J. Phys. Chem. B **106**, 3495 (2002).
[49] B. Ealet, J. Goniakowski, and F. Finocchi, forthcoming paper.